

Surface stress changes in the Ir(001)/H system: Density functional theory studyM. K. Bradley, D. P. Woodruff,^{*} and J. Robinson*Physics Department, University of Warwick, Coventry CV4 7AL, United Kingdom*

(Received 1 June 2011; published 8 August 2011)

Density functional theory calculations of the surface energy and surface stress changes associated with the formation of the Ir(001)(5×1)-hex clean-surface reconstruction and its transformation to a (5×1)-added row (AR) structure in the presence of adsorbed atomic hydrogen have been performed and compared with experimental results. The calculations clearly show that the clean-surface (1×1)-to-(5×1)-hex reconstruction is not driven by a reduction in tensile surface stress. While the surface energy is reduced by this transformation, the surface stress increases; proper convergence of the calculated surface stress requires the use of slabs containing at least nine atomic layers, due to the substantial subsurface relaxations associated with the (5×1)-hex phase. By contrast, the H-induced reconstruction leads to a calculated reduction in the tensile surface stress in the range 1.76–2.06 Nm^{-1} for an H coverage range of 0.6–0.8 ML, in excellent agreement with the experimentally determined value of 1.7 Nm^{-1} .

DOI: [10.1103/PhysRevB.84.075438](https://doi.org/10.1103/PhysRevB.84.075438)

PACS number(s): 68.35.Rh, 68.35.B-, 68.43.Fg

I. INTRODUCTION

Reconstruction of solid surfaces, in which atoms in the outermost layer(s) undergo lateral movements or even atomic density changes, relative to an ideal bulk termination, occurs in many systems. Even at the surfaces of metals, in which the bonding is predominantly nondirectional, there are examples of both clean-surface and adsorbate-induced reconstructions. Of course, the equilibrium structure of surfaces is determined by the minimization of the surface free energy, but the role of one contribution to the energy, the relief of surface stress, has often been invoked in trying to identify the driving force for these reconstructions. Unfortunately, quantitative information about surface stress and surface stress changes is sparse. Indeed, there is no experimental method capable of determining the absolute surface stress of a single-crystal surface, although there are a few measurements of the change in surface stress associated with a surface reconstruction and particularly with adsorbate-induced reconstructions. These measurements exploit the slight bending of a thin crystal beam, which occurs when the surface stresses on the two opposite faces are different; a variety of methods have been used to measure these changes in the crystal curvature associated with adsorption onto one face of the crystal (e.g. Ref. 1). The limited amount of experimental data of this kind has been supplemented by theoretical calculations with early examples of results for clean metal surfaces and adsorption upon them being reported by Needs and Mansfield,² and by Feibelman,³ respectively; a review of most of this earlier work was provided by Haiss.⁴

The Ir(001) surface is a particularly interesting system in that not only does the clean surface reconstruct to a (5×1)-hex structure, in which the outermost layer has a 20% increase in atomic density (with one extra atomic row in every five substrate spacings) to produce an approximately hexagonal close-packed surface^{5–7} (Fig. 1), but adsorption of hydrogen on this surface leads to a new reconstruction, also having a (5×1) unit mesh. However, this hydrogen-induced surface has an added-row (AR) structure⁸ (Fig. 1) in which single [110] rows of Ir atoms with a periodicity of $5 \times$ the nearest neighbor distance, lie on an otherwise unreconstructed (001) surface layer. This hydrogen-induced

transformation from the (5×1)-hex structure to the (5×1)-AR structure is one of the very few surface reconstructions for which there exists an experimental determination of the surface stress change, and indeed the measured (compressive) stress change is consistent with a probable lowering of the absolute value of the surface stress (which is believed to be invariably tensile for clean unreconstructed metal surfaces).⁹ The primary objective of the work reported here is to gain a description of these structures and the associated surface stress change using density functional theory (DFT) calculations and particularly to provide a comparison with this experimental measurement. In addition, however, we also report new DFT results of the computed surface stress changes associated with the reconstruction of the ideal bulk-terminated Ir(001) (1×1) surface to the Ir(001)(5×1)-hex phase. Equilibrium structures in which the outermost surface of a clean metal surface comprises a close-packed hexagonal layer are not only a feature of Ir(001), but also of Au(001), Au(111), Pt(001), and Pt(111). In all cases, the reconstruction has been attributed to relief of particularly high tensile stress in the ideal (1×1) bulk-terminated surface due to relativistic effects in these 5d metals.^{1,10} In the case of Ir(001), this interpretation was also arrived at from consideration of the measured surface phonon bands at the surface.¹¹ More recent DFT calculations of the surface stress change between the Ir(001)(1×1) and Ir(001)(5×1)-hex phases, however, have led to the conclusion that there is no significant change in the average surface stress and that surface stress relief is therefore not the key reason for the reconstruction.^{12,13} In fact our present calculations show that this transition is associated with an increase in the average tensile surface stress, although there is a reduction in the surface energy, consistent with the fact that the surface does reconstruct. For the hydrogen induced transformation to the Ir(001)(5×1)-AR structure, however, we do find a significant reduction in the tensile surface stress consistent with the experimental result.

II. COMPUTATIONAL DETAILS

The DFT calculations reported here were conducted using the plane-wave pseudopotential computer code CASTEP

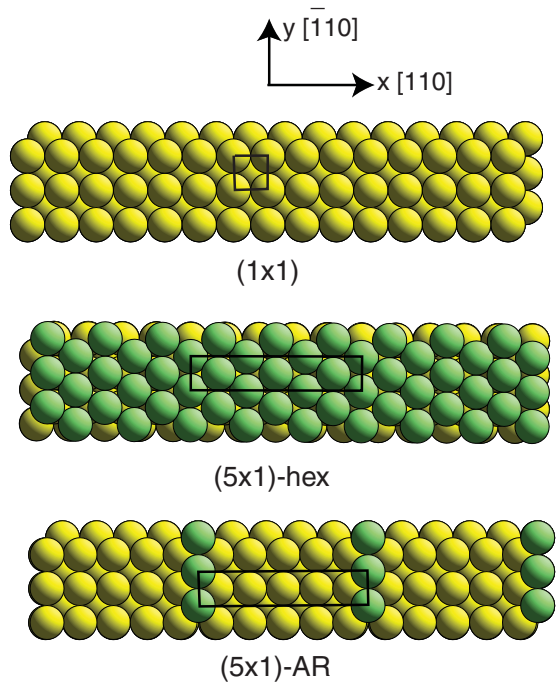


FIG. 1. (Color online) Schematic diagram of the Ir(001) clean-surface models discussed in the text, showing the definition of azimuthal directions used in this paper. The Ir atoms in the outermost layer in the hex reconstruction and in the adatoms of the AR structure are shown with a different shading (color) for clarity.

5.501.¹⁴ The RPBE (Revised Perdew-Burke-Ernzerhof) exchange-correlation functional¹⁵ was used throughout along with ultrasoft pseudopotentials. A plane-wave cutoff energy of 380 eV provided adequate basis set convergence, and a relatively dense 4×16 Monkhorst-Pack k -point mesh (16 k points in the irreducible Brillouin zone) was needed, along with a Hellmann-Feynman force tolerance of 0.01 eV/Å, to provide well-converged surface stresses in the (5×1) double-sided surface slabs considered in the study. Note that calculations of the bulk-terminated unreconstructed (1×1) surface were also performed using a (5×1) supercell to ensure identical k -point sampling and thus reliable comparability of surface energies and surface stresses with those of the reconstructed surfaces. Calculations were performed on seven-, nine-, and 11-layer

slabs, the outermost of these layers (on both sides) being either a (1×1) phase, a hexagonal layer, or a relaxed (1×1) -type layer plus one extra added row. In all cases, the middle three layers of these slabs were constrained to the calculated bulk fcc Ir structure with a lattice parameter of 3.906 Å, while a vacuum region of at least 8.5 Å was used to ensure minimal interaction between slabs.

In order to compare the relative energies of different surface structures (with and without adsorbed atomic hydrogen), surface energies of the double-sided slabs are defined as

$$E_{\text{surf}} = \frac{1}{2A} \left(E_{\text{slab}} - N_{\text{Ir}} E_{\text{bulk}} - \frac{1}{2} N_H E_{H_2} \right)$$

where A is the surface area of the computed supercell, N_{Ir} and N_H are the total number of the Ir and H atoms in this cell, E_{bulk} is the energy of an Ir atom within the bulk solid, and E_{H_2} is the energy of an isolated H_2 molecule. A smaller value of E_{surf} corresponds to a more favorable structure. For a clean surface (with $N_H = 0$), this corresponds to the normal definition of surface energy; for the hydrogen adsorption phases, this definition takes account of the energy gain (or loss) associated with H_2 dissociation combined with H adsorption and thus provides a means of identifying the overall energetic change associated with hydrogen adsorption. With both faces of the slabs having identical adsorbate coverage, the surface stress is the same on each face, and it is particularly trivial to extract this quantity from the calculated three-dimensional stress tensor, computed within CASTEP according to the so-called stress theorem.^{16,17}

III. RESULTS AND DISCUSSION

A. Clean surfaces

Table I summarizes the main results of the calculations for the clean-surface structures, namely the (1×1) bulk termination, the (5×1) -hex structure, and a (5×1) -AR structure with no H adsorbates. The results are shown for three different slab thicknesses, and while the differences in surface energy for these different slab thicknesses are modest, the changes in calculated surface stress are more significant. In particular, there are quite significant differences (up to 16%) between the results for the seven-layer and nine-layer slabs, but the additional change in increasing the thickness to 11 layers

TABLE I. Calculated surface energy and surface stress values for clean double-sided slabs of varying thickness for three different surface phases. The surface energy is given in units of eV per (1×1) unit mesh. S_x and S_y are the surface stress components in the long $[110]$ and short $[\bar{1}10]$ directions (Fig. 1) of the (5×1) unit mesh, respectively. S_{av} is the mean of the two stress components.

| Model | Layers | E_{surf} [eV/(1×1)] | S_x (Nm ⁻¹) | S_y (Nm ⁻¹) | S_{av} (Nm ⁻¹) |
|-----------------------------|--------|---|---------------------------|---------------------------|------------------------------|
| Ir(001)(1×1) | 7 | 1.369 | 3.38 | 3.34 | 3.36 |
| Ir(001)(1×1) | 9 | 1.359 | 3.45 | 3.43 | 3.44 |
| Ir(001)(1×1) | 11 | 1.364 | 3.51 | 3.52 | 3.51 |
| Ir(001)(5×1)-hex | 7 | 1.311 | 2.78 | 5.38 | 4.08 |
| Ir(001)(5×1)-hex | 9 | 1.308 | 3.23 | 5.70 | 4.47 |
| Ir(001)(5×1)-hex | 11 | 1.311 | 3.28 | 5.75 | 4.51 |
| Ir(001)(5×1)-AR | 7 | 1.398 | 2.22 | 3.46 | 2.84 |
| Ir(001)(5×1)-AR | 9 | 1.393 | 2.29 | 3.59 | 2.94 |
| Ir(001)(5×1)-AR | 11 | 1.392 | 2.31 | 3.58 | 2.94 |

is much smaller ($<3\%$). This effect is much larger for the (5×1) -hex structure than for the other two structures. The clear need to take at least nine layers (three fixed at the center, plus three relaxed on each face) to achieve reasonable convergence for this (5×1) -hex phase is consistent with previous findings of both low energy electron diffraction (LEED) experiments⁸ and DFT calculations^{18,19} that this reconstruction leads to structural changes in up to three subsurface layers. In checking the convergence of surface stress with slab thickness, we note that the calculated values are extremely sensitive to the lattice parameter used to define the lateral periodicity of the supercell. Calculations on a clean Ir $\{100\}$ - (1×1) unit mesh of varying slab thickness showed that a lattice parameter increase of just 0.001 \AA produces an artificial increase in apparent surface stress of 0.05 Nm^{-1} per additional pair of substrate layers. The reason is clear; if the lattice parameter is wrong, the bulk material is stressed, so adding layers increases the total stress in the slab, and this is interpreted in our calculations as being due entirely to stress at the two surfaces. The fact that our calculated surface stress values do converge with increasing thickness indicates that this has little or no influence on our results, though we also note that any residual error due to this effect does not affect our calculation of relative stresses for slabs containing the same number of layers but different surface structures.

Table I shows that the surface energy of the (5×1) -hex structure is lower than that of the unreconstructed (1×1) surface, consistent with the experimental observation that this transformation occurs, although the energy difference is only 0.05 eV per (1×1) unit mesh. This value is similar to those reported in previous DFT studies using the LDA (local density approximation) and GGA-PW91 (generalized gradient approximation - Perdew-Wang exchange and correlation) functionals that gave values of 0.14 eV ¹² and 0.05 eV ,¹⁹ respectively. Table I also shows, however, that the average tensile surface stress actually increases in this transformation to the hex phase; this reinforces the more recently held view that surface stress relaxation cannot be the driving force for the reconstruction.^{1,12} The only previous surface stress DFT calculation for this transformation reported that there was no significant change,¹² but this calculation was performed using only a five-layer slab, so our results indicate that this was unlikely to be properly converged. In fact, our calculations show that the surface stress in the $[110]$ ($5 \times$) direction of the surface unit mesh (S_x) is reduced slightly, but that in the $[\bar{1}10]$ ($1 \times$) direction (S_y) is increased rather substantially.

While the calculations provide clear answers regarding the predicted changes in surface stress, interpreting these changes in terms of simple physical processes is potentially complex. For free-electron-like metals, a particularly simple picture can be derived from a jellium model, in which the tensile surface stress of a clean unreconstructed surface is attributed to the electron charge spillover into the vacuum and a resulting depletion of such charge in the surface layer; within a density functional formalism, this means attributing the effect to the change in the kinetic energy contribution.^{20,21} For d-band metals, the situation is more complex with the role of the localised d electrons, in particular making a picture based on interatomic bonds and bond coordination more relevant.¹⁰ However, a recent computational study of the surface stress

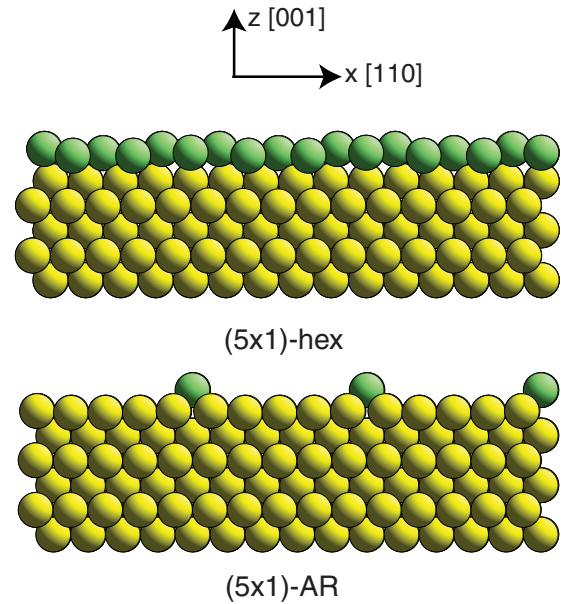


FIG. 2. (Color online) Schematic side views of the Ir(001) (5×1) clean-surface models shown in Fig. 1. The exact geometry is that corresponding to the minimum total energy in 11-layer DFT calculations, as described in the text.

of a wide range of d-band metals indicates that for the late elements in the 5d series and particularly for Ir, the charge spillover is the dominant contribution.²² We therefore discuss our results within this simple picture, but may note that an alternative interpretation in terms of local bonding can also be shown to be qualitatively consistent with our results.

The small decrease in the stress associated with the $(1 \times 1) \rightarrow (5 \times 1)$ -hex phase in the $[110]$ direction can then be seen to be qualitatively consistent with our expectation that packing in an extra Ir atomic row and reducing the atom spacing in this direction should increase the electron charge density and reduce the tensile stress. By contrast, the much larger increase in the $[\bar{1}10]$ direction, in which the atomic spacing is unchanged, is at first sight surprising. However, we note that the pseudohexagonal surface layer is heavily rumpled (see Fig. 2), causing the average spacing of this layer to the underlying unreconstructed layer to be significantly larger than in the (1×1) termination. This average outward shift places the surface layer in a region of depleted valence charge from the underlying surface, and this can be expected to increase the surface stress. In view of this, the rather small decrease in tensile stress in the $[110]$ direction can be seen as due to a near balance of two competing processes.

In order to provide further clarification of these underlying mechanisms, additional surface stress calculations were performed for a number of fixed model structures. In one of these, the minimum-energy (5×1) -hex structure was changed only by increasing the layer spacing of the reconstructed surface layer relative to the underlying bulk. An increase in this spacing of only 0.1 \AA led to new values for S_x and S_y of 5.18 and 7.43 Nm^{-1} , increases of 1.90 and 1.68 Nm^{-1} , respectively, providing clear confirmation of the influence of increasing the layer spacing. In a second model, the rumpling of the

reconstructed hex layer was removed, but the average inter-layer spacing of the minimum-energy structure retained. This calculation yielded values for S_x and S_y of 0.54 and 5.42 Nm^{-1} . The value of S_y in this unrumped model structure is very similar to that of the equilibrium rumped structure, indicating that in this direction the stress is predominantly determined by the average layer spacing. By contrast, the value of S_x in this unrumped model structure is much lower than in the rumped structure; removing the rumpling increases the linear packing density along [110] and thus relieves the tensile stress in this direction more effectively. The results of further calculations using different layer spacings confirm this pattern of behavior, while calculations for isolated surface layers (with the substrate removed) led to very large increases in tensile stress due to the further depletion of valence surface charge within the layer.

The results for the (5×1) -AR clean surface structure are also consistent with this simple picture. Note that the surface energy of this structure is higher than either the (1×1) or the (5×1) -hex phases, consistent with the fact that this structure does not occur in the absence of adsorbed hydrogen. In this model, the outermost surface layer has a structure closely similar to that of the (1×1) termination with an almost ideal bulk-termination, but for the addition of a single added row with a $5 \times$ periodicity (Fig. 2). A modest reduction in S_x may be attributed to an increase in the average valence charge density within the outermost (1×1) layer due to electrons coming from the adatom row after Smoluchowski smoothing. The value of S_y is very similar to that of the (1×1) phase, a result that may be attributed to a combination of the reduction in the tensile stress in the outermost complete layer as for S_x , but a contribution of higher tensile stress from the atoms in the added row which have a greatly depleted valence charge density.

B. Hydrogen adsorption

In order to calculate the surface stress changes associated with the hydrogen-induced (5×1) -AR structure, one needs to establish two things, namely the H coverage and the H adsorption site(s). Within the (5×1) -AR surface unit mesh, there are a large number of possible individual sites, and as the H coverage is likely to be greater than 0.2 ML (i.e. greater than one H atom per unit mesh), there is an even larger number of possible combinations of different sites that might be occupied. Nevertheless, our calculations for 12 different singly occupied sites showed that threefold and fourfold coordinated sites were unstable, the H atoms moving to atop or bridging sites. The properties of the eight stable top and bridging sites are shown in Table II. Establishing the relative energies of multiple occupation of the many different combinations of sites (of up to four H atoms per unit mesh, a coverage of 0.8 ML), however, is a formidable computational task, but a recent publication²³ has reported the results of such an investigation using a novel approach to reduce the computational demands. Several of these results have also been reproduced more recently by Vukajlovic *et al.*²⁴ Our results for the single sites are fully consistent with the results of this recent paper, as are our conclusions regarding the most favorable combinations of sites. Figure 3 shows the labeling convention we have used for these bridge and top sites, while Table II summarizes the results of calculations for seven-layer double-sided slabs. In this table, we not only give the surface stress values and the surface energy per (1×1) unit mesh, as defined above, but also the adsorption energy per H atom, E_{ad} . This is defined as $E_{ad} = \frac{1}{N}(E_{\text{clean-slab}} + \frac{1}{2}N_H E_{H_2} - E_{H\text{-adsorbed-slab}})$ such that the highest positive value corresponds to the strongest adsorbate bonding.

TABLE II. Adsorption energies, E_{ad} , and surface energies, E_{surf} , (as defined in the text) and surface stress values calculated for different H adsorption structures on the Ir(001) (5×1) -AR surface structure. All results are for seven-layer slabs apart from the bracketed values in the last two rows, which are for 11-layer slabs.

| Model | Coverage (ML) | E_{ad} (meV) | E_{surf} [eV/(1×1)] | S_x (Nm^{-1}) | S_y (Nm^{-1}) | S_{av} (Nm^{-1}) |
|-----------------------------|---------------|----------------|---|----------------------------|----------------------------|-------------------------------|
| Ir(001) (5×1) -hex | | | | | | |
| 1H | 0.2 | 337 | 1.244 | 2.11 | 4.71 | 3.41 |
| 2H | 0.4 | 318 | 1.184 | 2.41 | 4.22 | 3.31 |
| 3H | 0.6 | 307 | 1.127 | 1.94 | 3.28 | 2.61 |
| Ir(001) (5×1) -AR | | | | | | |
| Tad | 0.2 | 491 | 1.301 | 2.13 | 2.88 | 2.50 |
| Tb | 0.2 | 506 | 1.298 | 2.05 | 3.14 | 2.59 |
| Tc | 0.2 | 509 | 1.297 | 2.01 | 3.22 | 2.62 |
| Badad | 0.2 | 798 | 1.239 | 2.36 | 3.77 | 3.06 |
| Bab | 0.2 | 478 | 1.303 | 2.05 | 2.90 | 2.48 |
| Bbc | 0.2 | 657 | 1.267 | 2.16 | 2.95 | 2.56 |
| Bbb | 0.2 | 656 | 1.268 | 1.78 | 3.39 | 2.59 |
| Bcc | 0.2 | 680 | 1.263 | 1.69 | 3.45 | 2.57 |
| Badad + Bcc | 0.4 | 740 | 1.103 | 1.82 | 3.73 | 2.78 |
| Badad + 2xBbb | 0.6 | 708 | 0.974 | 1.51 | 3.82 | 2.67 |
| Badad + Bbb + Bcc | 0.6 | 717 | 0.968 | 1.39 | 3.77 | 2.58 |
| | | [715] | [0.963] | [1.55] | [3.92] | [2.74] |
| Badad + 2xBbb + Bcc | 0.8 | 707 | 0.833 | 0.80 | 3.70 | 2.25 |
| | | [704] | [0.829] | [0.99] | [3.91] | [2.45] |

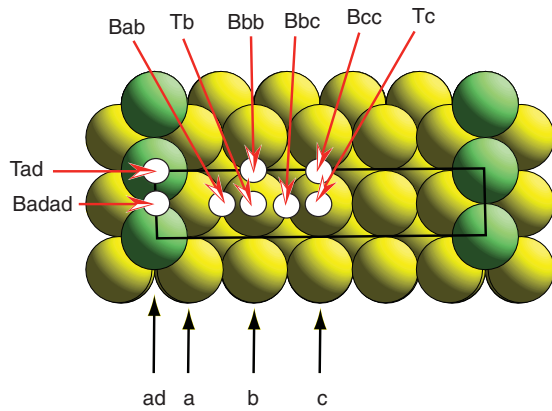


FIG. 3. (Color online) Schematic diagram of the Ir(001)(5×1)-AR surface structure with a number of sites for H adsorption labeled. Bridge sites are labeled B followed by the labels of the rows occupied by the nearest neighbor Ir atoms [ad (adatom), a, b, or c]. Top sites are labeled T followed by the label of the row occupied by the underlying single nearest-neighbor Ir atom.

In addition to calculations for H adsorption on the (5×1)-AR structure reported in Table II, a few results are included for adsorption on the (5×1)-hex phase, using the (sequentially filled) preferred threefold coordinated adsorption sites, previously identified in DFT calculations by Lerch *et al.*,¹⁹ and in the earlier combined LEED/DFT study of Poon *et al.*²⁵ The associated adsorption energies provide a further check on our results and are found to be closely similar to the earlier published values.¹⁹ Our values are approximately 60 meV/atom smaller (before application of the small correction for the vibrational ground-state energy included in this earlier work), a difference that may be due to the different (GGA-PW91) functional used by Lerch *et al.*

Comparison of our calculated H adsorption energies with those of the previous study in the (5×1)-AR surface²³ shows the same behavior with the ordering of the preferred single adsorption sites, namely Badad > Bcc > Bbc > Bbb > Tad > Tc > Tb > Bab being identical to that of this earlier study. Comparison of the surface energies given in Table II for H adsorption on the (5×1)-hex and (5×1)-AR structures shows that even for the lowest coverage of 0.2 ML [one H atom per (5×1) unit mesh], there is a small energetic advantage to reconstruction to the (5×1)-AR phase with the H atoms adsorbed in the Badad site bridging nearest-neighbor Ir atoms in the adatom rows. This energetic advantage for the phase transition increases with increasing coverage.

Table II also shows that the combination of H adsorption and the associated transformation from the clean-surface (5×1)-hex phase to the hydrogen covered is accompanied by a significant reduction in the tensile surface stress. In this case, we have the possibility to compare this result with an experimental measurement which showed a total surface stress change of -1.7 Nm^{-1} for this same transition.⁹ Here, we should note that, because the Ir(001) surface has fourfold rotational symmetry, the anisotropy associated with a single rotational domain of any of the (5×1) surface phases cannot be measured. Instead, the surface comprises domains of (5×1) and (1×5) structures that are expected for an ideally

oriented (001) surface to be equally occupied. The experiment thus measures the average of the two orthogonal orientations and must be compared with our computed values of S_{av} . For the clean (5×1)-hex surface the value calculated for an 11-layer slab, 4.51 Nm^{-1} , is likely to be the most reliable. The appropriate value for the hydrogen-covered (5×1)-AR phase depends on the H coverage, but it has been reported that thermal desorption measurements indicate a coverage of 0.8 ML.²⁶

In our calculations for the surface stress of the clean-surface structures, we noted that the need to include at least nine layers in the computed slab was most acute for the (5×1)-hex surface due to the significant subsurface relaxations in this phase. On this basis, seven-layer slab calculations may suffice for the (5×1)-AR- H phase, but to minimize any possible errors, additional 11-layer slab calculations were performed for the energetically favored highest H -coverage structures. These are included in square brackets in Table II. The surface stress value for the 11-layer slab at an H coverage of 0.8 ML given in Table II is 2.45 Nm^{-1} , corresponding to a reduction from the clean surface of 2.06 Nm^{-1} , quite close to the experimental value. In view of the uncertainty in the H coverage, however, we may also note that a coverage of 0.6 ML our calculations predict a reduction in the tensile surface stress of 1.76 Nm^{-1} , even closer to the experimental value.

IV. CONCLUSIONS

The results of our DFT calculations for the Ir(001) surface provide some further insight into the role of surface stress in the clean and H -induced reconstructions. In the case of the clean surface (1×1) \rightarrow (5×1)-hex transition, our results reinforce the more recently held view that this transition does not reduce the surface tensile stress. Indeed, while the previous calculation indicated almost no change in the surface stress associated with this transformation, our calculations show that if the thickness of the slab used in the calculation is increased sufficiently to account fully for the subsurface relaxations of the (5×1)-hex phase, there is actually a significant increase (of $\sim 1.0 \text{ Nm}^{-1}$) in the tensile surface stress. Nevertheless, the surface energy is reduced, consistent with the fact that the (5×1)-hex phase is found to be the equilibrium structure. A previous experimental study of the H -induced transition to the (5×1)-AR phase, however, has shown that this transformation is accompanied by a reduction in the tensile surface stress of 1.7 Nm^{-1} , an effect reproduced in our theoretical calculations that show a closely similar value for the reduction of 1.76 – 2.06 Nm^{-1} , depending on the H coverage in the range 0.6–0.8 ML.

ACKNOWLEDGMENTS

The authors acknowledge the partial support of the Engineering and Physical Sciences Research Council (UK) for this work. The computing facilities were provided by the Centre for Scientific Computing of the University of Warwick with support from the Science Research Investment Fund.

*Corresponding author: d.p.woodruff@warwick.ac.uk

- ¹H. Ibach, *Surf. Sci. Rep.* **29**, 193 (1997).
- ²R. J. Needs and M. Mansfield, *J. Phys. Condens. Matter* **1**, 7555 (1989).
- ³P. J. Feibelman, *Phys. Rev. B* **56**, 2175 (1997).
- ⁴W. Haiss, *Rep. Prog. Phys.* **64**, 591 (2001).
- ⁵M. A. Van Hove, R. J. Koestener, P. C. Stair, J. P. Bibérian, L. L. Kesmodel, I. Bartos, and G. A. Somorjai, *Surf. Sci.* **103**, 218 (1981).
- ⁶L. Lang, K. Müller, K. Heinz, M. A. Van Hove, R. J. Koestner, and G. A. Somorjai, *Surf. Sci.* **127**, 347 (1983).
- ⁷A. Schmidt, W. Meier, L. Hammer, and K. Heinz, *J. Phys. Condens. Matter* **14**, 12353 (2002).
- ⁸L. Hammer, W. Meier, A. Klein, P. Landfried, A. Schmidt, and K. Heinz, *Phys. Rev. Lett.* **91**, 156101 (2003).
- ⁹D. Sander, Z. Tian, and J. Kirschner, *J. Phys. Condens. Matter* **21**, 134015 (2009).
- ¹⁰V. Fiorentini, M. Methfessel, and M. Scheffler, *Phys. Rev. Lett.* **71**, 1051 (1993).
- ¹¹J. G. Chen, S. Lehwald, G. Kisters, E. Preuss, and H. Ibach, *J. Electron Spectrosc. Relat. Phenom.* **54-55**, 405 (1990).
- ¹²A. Filippetti and V. Fiorentini, *Surf. Sci.* **377**, 112 (1997).
- ¹³H. Ibach, *Surf. Sci. Rep.* **35**, 71 (1999).
- ¹⁴S. J. Clark, M. D. Segall, C. J. Pickard, P. J. Hasnip, M. J. Probert, K. Refson, and M. C. Payne, *Z. Kristallogr.* **220**, 567 (2005).
- ¹⁵B. Hammer, L. B. Hansen, and J. K. Norskov, *Phys. Rev. B* **59**, 7413 (1999).
- ¹⁶O. H. Nielsen and R. M. Martin, *Phys. Rev. B* **32**, 3780 (1985).
- ¹⁷M. C. Gibson, *Implementation and Application of Advanced Density Functionals*, 14 Sep 2006, [http://cmt.dur.ac.uk/sjc/thesis_mcg/node117.html].
- ¹⁸D. Spišák and J. Hafner, *Surf. Sci.* **546**, 27 (2003).
- ¹⁹D. Lerch, S. Müller, L. Hammer, and K. Heinz, *Phys. Rev. B* **74**, 075426 (2006).
- ²⁰R. J. Needs and M. J. Godfrey, *Phys. Rev. B* **42**, 10933 (1990).
- ²¹M. Mansfield and R. J. Needs, *Phys. Rev. B* **43**, 8829 (1991).
- ²²M. Blanco-Rey and S. J. Jenkins, *J. Phys. Condens. Matter* **22**, 135007 (2010).
- ²³D. Lerch, O. Wieckhorst, L. Hammer, K. Heinz, and S. Müller, *Phys. Rev. B* **78**, 121405 (2008).
- ²⁴F. R. Vukajlovic, Z. S. Popovic, A. Baldereschi, and Ž. Šljivančanin, *Phys. Rev. B* **81**, 085425 (2010).
- ²⁵H. C. Poon, D. K. Saldin, D. Lerch, W. Meier, A. Schmidt, A. Klein, S. Müller, L. Hammer, and K. Heinz, *Phys. Rev. B* **74**, 125413 (2006).
- ²⁶A. Klein, Ph.D. thesis, University Erlangen-Nürnberg (2007), as reported in Ref. 23.